Process Safety and Environmental Protection 150 (2021) 478–488

Contents lists available at ScienceDirect

Process Safety and Environmental Protection

journal homepage: www.elsevier.com/locate/psep

Rapid gas desorption and its impact on gas-coal outbursts as two-phase flows

Aitao Zhou[a,b,c], Meng Zhang[a,b,d,*], Kai Wang[a,b,*], Derek Elsworth[c], Nan Deng[e], Jiaying Hu[a,b]

[a] Beijing Key Laboratory for Precise Mining of Intergrown Energy and Resources, China University of Mining and Technology (Beijing), Beijing, 100083, China
[b] School of Emergency Management and Safety Engineering, China University of Mining and Technology (Beijing), Beijing, 100083, China
[c] Department of Energy and Mineral Engineering, EMS Energy Institute and G3 Center, Pennsylvania State University, University Park, PA, USA
[d] Department of Mining Engineering, Yuncheng Vocational and Technical University, Yuncheng, 044000, China
[e] China Coal Research Institute, Beijing, 100083, China

ARTICLE INFO

Article history:
Received 26 February 2021
Received in revised form 19 April 2021
Accepted 27 April 2021
Available online 29 April 2021

Keywords:
Coal and gas outburst
Gas emission model
Contribution of desorption gas
Quantitative study
Outburst two-phase flow

ABSTRACT

Coal and gas outbursts are a violent release of energy in part driven by rapidly desorbing gas from the fragmenting coal. We present a coupled two-phase model of coal and gas outbursts to define the timing, rate and magnitude of gas desorption and its contribution to the resulting energetics. The model involves a fragmenting ejection of the outburst from an overpressurized coal that retreats omnidirectionally from a point and develops a deepening crater. This model is applied to represents both experiments and in situ observations. These results indicate that the outburst is initially driven by free gas before desorbing gas rate exceeds this free gas liberation rate early into the outburst (at ~17 s in our model). The cumulative mass of desorbed gas only exceeds the free gas later into the event at approximately double this duration (at ~29 s in our model). During the outburst, ~55 % of the expansion energy is contributed by desorbing gas. Using the initial gas emission rates for both non-tectonic and tectonic coals defines a power-law relationship between the initial gas desorption rate and the desorption gas contribution (~14 %–92 %), indicating that the desorbing gas plays a decisive role in outburst development. Furthermore, taking the gas emission model as a boundary conditions for numerical simulations, the gas pressure potential energy (GPPE) released in the first millisecond at the maximum gas emission rate is derived to characterize its effects on the dynamic characteristics of the outburst two-phase flow. The maximum energy release intensity considering gas desorption is ~5 times that without gas desorption for non-tectonic coal. For tectonic (mylonitized) coals the energy release is a further ~4 times greater than that of non-tectonic coals. This paper presents a novel quantitative study defining the role of gas desorption in outbursts and contributes to the understanding of causal mechanisms and precursory phenomena preceding catastrophic outbursts.

1. Introduction

Coal and gas outbursts are one of the major hazards in underground coal mining and greatly restrict the safe recovery of the resource (Díaz Aguado and González Nicieza, 2007; Karacan et al., 2011; Zhang et al., 2020). Outbursts are a dynamic phenomenon in which a mixture of coal and gas are ejected into the working space within a very short time - potentially causing serious casualties and economic loss (Chen et al., 2012). The attributes of the phenomenon are typified by the following aspects (Lama and Bodziony, 1998; Li et al., 2015; Sun et al., 2018; Fu et al., 2020):

I The gas-solid mixture is ejected at high-speed and compresses the air in the roadway and forms a shock wave. At the wave-front, the physical characteristics (gas density, pressure and solids concentration) of the medium change drastically and this has severe consequences to personnel, equipment and facilities.
II In the working space, where the outburst occurs, the fast-moving coal mass impacts and buries equipment and personnel.

* Corresponding authors at: School of Emergency Management and Safety Engineering, China University of Mining and Technology (Beijing), Beijing, 100083, China.
E-mail addresses: mzhang_cumt@163.com (M. Zhang), safety226@126.com (K. Wang).

https://doi.org/10.1016/j.psep.2021.04.042
0957-5820/

Simultaneously, the large volume of gas at high-concentrations may result in the suffocation of personnel and gas overrun.

III The shock-wave airflow entrains a large mass of gas into the ventilation network. Not only will a dynamic gas pressure be generated in inclined roadways, but also the gas concentration in the affected area may exceed the explosive limit and result in a secondary gas explosion.

Coal and gas outbursts are a process of violent energy release resulting the propelling of the mixture at a high speed and potentially resulting in serious damage (An et al., 2019; Rudakov and Sobolev, 2019). It is generally accepted that outbursts result from the combined action of gas, in-situ stress and coal strength (Beamish and Crosdale, 1998; Liu et al., 2018). Quantitative analysis of the ejected coal mass and the released gas shows that the energy provided by the gas is 1–3 orders of magnitude greater than that provided by the in-situ stress through stored strain energy. Additionally, in the development of outbursts, the coal seam is destroyed, and the in-situ stresses are substantially released. Therefore, the energy for this stage must be mainly derived from the gas in the coal mass (Wang et al., 2019). According to process-following experiments, the temperature drop in the outburst chamber is ~2 °C (Nie et al., 2019) and only ~0.3 °C in simulated roadways (Sun et al., 2018). The major energy is not from the internal energy of gas. Thus, it is clear that the energy consumed in gas expansion represents a significant energy source in the development stage (Guan et al., 2009; Zhao et al., 2017) and can therefore not be neglected.

The gas reservoir within the coal seam includes both free and adsorbed gas. As outbursts evolve, coal spallation retreats rapidly within an outburst crater (Tu et al., 2018). Under the joint action of gas pressure gradient and collision, coal pulverization is further intensified. At the same time, the free gas in the pore and fracture space and desorbing gas in the coal matrix are released to provide energy to sustain the development of the outburst (Zhao et al., 2019). Of course, gas desorption takes a finite time, and a typical outburst lasts only for tens of seconds, during which time the desorbed gas participates in the propagation of the outburst as a two-phase flow (Zhi and Elsworth, 2016). Simulated experiments with CO_2 and N_2 (Jin et al., 2018) show that the eff ;ect of gas desorption may increase total energy by 1.30~2.43 times - the contribution of the energy provided by gas desorption may be of the order of ~56 %. The energy involved in outbursts with CO_2 is ~5.8 times larger than the energy involved in outbursts with air, which is mainly due to the different gas adsorption capacity (Cao et al., 2019). However, to make such a contribution (Zhao et al., 2016), rapid desorption must occur from small particles with critical particle sizes (TCPS) defined for the Zhongliangshan outburst defined as of the order of ~117 μm. Numerical simulations (Zhou et al., 2018) have defined the propagation characteristics for outbursts based on gas desorption - derived from experiments with coal particles of various sizes. These studies reveal that coal pulverization significantly accelerates gas desorption rate and that gas desorption plays an important role in the development and sustaining of outbursts. However, prior studies mostly analyze the contribution of desorbing gas from the perspective of energy, or obtain empirical gas release laws from desorption tests, rather than accurately and directly quantifying the gas emission from the outburst.

We develop an understanding of gas emission (inclusive of both free and desorbed gas) based on a theoretical model of coal-gas outbursts to define the contribution of desorbing gas and its effects on the outburst-driven two-phase flow. This model is then applied against quantitative measurements from tests at the Zhongliangshan mine. Though this model, the scope of the disaster can be predicted more accurately, providing guidance for the design of outburst prevention equipment and emergency rescue. Moreover, this study provides a quantitative method to characterize the contribution and role of desorbed gas in outbursts, improving causal mechanisms of catastrophic outbursts.

2. Theoretical calculation of gas emission rate in outbursts

High-pressure gas accumulated in the coal seam is released once an outburst initiates. Not all of the gas is released immediately to participate in the outburst, as the dynamic phenomenon lasts for tens of seconds, and the gas desorption takes a finite amount of time – requiring that this delay is quantified to determine whether desorbing gas may indeed make a significant contribution.

2.1. Analysis of gas sources in outbursts

At current mining depths in China, the gas content within the coal seam is generally within 15~ 40 m^3/t (Hu and Wen, 2013). Accident statistics show that gas emissions per ton of coal are higher than the coal seam gas contents in most coal and gas outburst accidents and may reach up to ten times the coal seam gas content in some cases. For example, on August 23, 2005, a catastrophic coal-gas outburst occurred in the Jiulishan coal mine (Wang and Zhou, 2014), in which the mass of coal entrained in the outburst was 2887.15 t while the outburst gas volume reached 279,000 m^3 (i.e. ~97 m^3/t). Thus, the gas emission per ton of coal was much higher than the maximum in situ gas content of 33.19 m^3/t in the mining coal seam. Clearly, the gas emission is sourced not only from the ejected coal, but also from the coal mass around the outburst crater.

In the formation of outburst crater, coal fragments are continuously stripped from the crater-intact-coal boundary and the coal and rock mass around the hole are exposed to continued deformation under the action of the original rock stress, impact dynamics and gas seepage, causing damage or even fracture (Cao et al., 2020). Due to the anticipated increase in porosity and permeability in the damaged coal mass, a large amount of gas will desorb and be rapidly liberated (Fedorchenko and Fedorov, 2012). The outburst intensity and the geological conditions local to the outburst control the increase in the permeability of the coal mass around the outburst crater. This is why gas emissions per ton of coal increase exponentially relative to original gas content during the outburst – proportionally to the crater wall area. Therefore, the gas emitted during and after the outburst are sourced both from the coal ejected during the outburst and the freshly exposed face around the outburst crater. Thus, gas emission rates may be recorded as q_1 and q_2, respectively (Fig. 1). Then the total gas emission rate q during the outburst can be expressed as,

$$q = q_1 + q_2 + q_3 \tag{1}$$

where q_1 and q_2 represent gas emission rates from the ejected coal and the outburst crater wall, m^3/s; q_3 is the gas emission rate from coal face under normal conditions, m^3/s. q_3 is generally much smaller than q_1 and q_2, and can be neglected.

2.2. Emission rate of gas from the outburst coal

Key from the foregoing is the necessary to establish a physical model to relate the gas emission from the ejected coal with the amount of coal ejected and its timing during and after the outburst. Outburst craters usually present special shapes, such as pear-shaped, the shape of an inverted bottle and ellipsoidal (Sun et al., 2012; Fisne and Esen, 2014). For convenience, simplicity of calculation and to add generality to the model, we assume an ellipsoidal outburst crater.

During the outburst, the gas emission rate of the ejected coal will change with the increase of the ejected coal volume. Thus, we

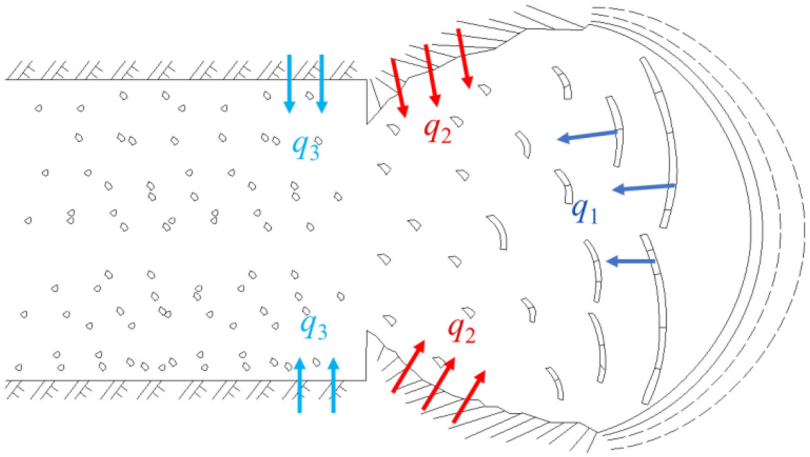

Fig. 1. Schematic diagram of gas emission sources during outbursts.

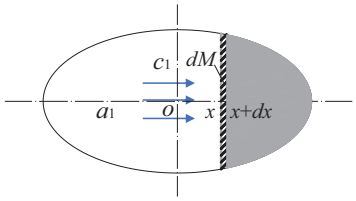

Fig. 2. Cross sectional view of an idealized evolving outburst crater.

analyze how the volume of the outburst crater changes with the advance of the outburst. It is assumed that the duration of the outburst is t_0, and that the outburst crater gradually develops from a small ellipsoid to a larger but self-similar ellipsoid within time t_0. The crater evolves from and to a single ellipsoid with a major axis radius of a_1 and minor axis radii of b_1 and c_1 (Fig. 2). It is further assumed that the outburst crater is formed at a constant speed along the major axis direction from the leftmost end of the axis. Thus, the average speed of formation is $2a_1/t_0$. At a certain time t ($t \le t_0$) during the duration of the outburst, the position x where the rim of the outburst crater reaches can be expressed as Eq. (2).

$$x = \frac{2a_1 t}{t_0} - a_1. \tag{2}$$

At $t=0$, the length of the major axis of the outburst hole is 0; while at $t=t_0$, it is a_1. So the change in the mass of ejected coal dM can be written as Eq. (3).

$$dM = \frac{\pi b_1 c_1 \rho}{a_1^2}\left(a_1^2 - x^2\right)dx = \frac{8\pi a_1 b_1 c_1 \rho}{t_0^2}\left(t - \frac{t^2}{t_0}\right)$$
$$dt = \frac{6M}{t_0^2}\left(t - \frac{t^2}{t_0}\right)dt \tag{3}$$

where ρ is the density of the coal, t/m^3, and M is the outburst intensity at time t, defined as a mass of coal entrained in the outburst.

It is assumed that for the mass of coal ejected, dM, all the free gas in the pores is released instantly and the adsorbed gas is continuously desorbed. When the outburst develops to time t, coal with a total mass of $M(t)$ is thrown out, but gas is emitted at different rates from the coal mass $M(t)$. For the a mass of coal $dM(\tau)$ ejected from τ ($\tau < t$) to $\tau+d\tau$, the gas desorption rate q_{ad} is expressed through a Winter model as:

$$q_{ad} = v_1 t^{-K_n} \tag{4}$$

where v_1 is the initial gas desorption rate from the coal with the rate in the first one second adopted, cm^3/ (g· s); K_n is the attenuation coefficient, obtained as

$$Q_{con} = v_1 + \int_1^{+\infty} q_{ad}dt = \frac{K_n}{K_n - 1}v_1 \tag{5}$$

where Q_{con} is the gas content, cm^3/g.

According to Eq. (4), the desorption gas rate of the outburst coal during the period from τ to $\tau+d\tau$ is $v_1 dM(\tau)$, and it decays to v_1 (t-τ+1) $^{-Kn}$ $dM(\tau)$ at time t. Then, for coal with a mass of $M(t)$ ejected before time t, the desorption gas emission rate can be expressed as:

$$q_{ad} = \int_{M(t)} v_1 (t - \tau + 1)^{-K_n} dM(\tau)$$
$$= \frac{6Mv_1}{t_0^2}\int_0^t (t - \tau + 1)^{-K_n}\left(\tau - \frac{\tau^2}{t_0}\right)d\tau \tag{6}$$

When the outburst ends, i.e., $t > t_0$, the desorption gas rate can be expressed as:

$$q_{ad} = \frac{6Mv_1}{t_0^2}\int_0^{t_0} (t - \tau + 1)^{-K_n}\left(\tau - \frac{\tau^2}{t_0}\right)d\tau \tag{7}$$

Using integration by parts, the desorption gas emission rate of the coal ejected during the entire outburst process is:

$$q_{ad} = \begin{cases} \dfrac{6Mv_1}{t_0^2}\left[\dfrac{t - t^2/t_0}{K_n - 1} - \dfrac{(t+1)^{2-K_n} - \left(1 - 2t/t_0\right)}{(K_n - 1)(2 - K_n)}\right. \\ \left. + \dfrac{2(t+1)^{3-K_n} - 2}{(K_n - 1)(2 - K_n)(3 - K_n)t_0}\right], t \le t_0 \\ \dfrac{6Mv_1}{t_0^2}\left[\dfrac{2(t+1)^{3-K_n} - 2(t - t_0 + 1)^{3-K_n}}{(K_n - 1)(2 - K_n)(3 - K_n)t_0}\right. \\ \left. - \dfrac{(t - t_0 + 1)^{2-K_n} + (t+1)^{2-K_n}}{(K_n - 1)(2 - K_n)}\right], t > t_0 \end{cases} \tag{8}$$

For the free gas released from the ejected coal, when $t \le t_0$, this can be expressed as:

$$q_f = \frac{p_m \phi_m}{p_0 \rho}\frac{dM}{dt} = \frac{p_m \phi_m}{p_0 \rho}\frac{6M}{t_0^2}\left(t - \frac{t^2}{t_0}\right) \tag{9}$$

where p_m is the gas pressure in the coal seam, MPa; ϕ_m is the porosity of the coal; ρ is the density of the coal, t/m^3; and p_0 is the

Table 1
Example verifications of gas outburst emission results.

Accident location	Date	Gas emission volume from the outburst coal (m^3)	Gas emission volume from the outburst hole wall (m^3)	Total gas emission volume (m^3)		
				Calculated value	Measured value	Error
Zhongliangshan Coal Mine	1977.11.4	13892.28	22062.59	35954.87	38540	6.7%
Pingdingshan 8# Mine	1995.5.28	633.1769	1300.87	1934.05	2142	9.7%
Well 1 of Nantong Coal Mine	1969.4.18	85356.95	984793	1070149.95	1250000	14.38%
Tangjiachong Mine, Hunan	1991.3.24	20089.156	131179.9	151269	145000	4.32%
Meitian Mining Bureau 2# Mine, Gunagdong	1977.8.3	6567.65	137991.3	144558.65	150000	3.63%
Zhucun Mine, Henan	2003.1.23	9268.35	40721.37	49989.72	51674	3.26%
Well 1 of Nantong Coal Mine	2002.1.31	16453.6	176170.9	192624.5	200000	3.69%

atmospheric pressure, MPa. The gas emission from outburst coal is the sum of desorbed gas and free gas emission, namely:

$$q_1 = \begin{cases} \dfrac{6Mv_1}{t_0^2}\left[\dfrac{t-t^2/t_0}{K_n-1} - \dfrac{(t+1)^{2-K_n}-\left(1-2t/t_0\right)}{(K_n-1)(2-K_n)} + \dfrac{2(t+1)^{3-K_n}-2}{(K_n-1)(2-K_n)(3-K_n)t_0}\right] \\ \quad + \dfrac{p_m\phi_m}{p_0\rho}\dfrac{6M}{t_0^2}\left(t-\dfrac{t^2}{t_0}\right), t \le t_0 \\ \dfrac{6Mv_1}{t_0^2}\left[\dfrac{2(t+1)^{3-K_n}-2(t-t_0+1)^{3-K_n}}{(K_n-1)(2-K_n)(3-K_n)t_0} - \dfrac{(t-t_0+1)^{2-K_n}+(t+1)^{2-K_n}}{(K_n-1)(2-K_n)}\right], t > t_0 \end{cases} \tag{10}$$

2.3. Prediction of total gas emission rate in outbursts

As the outburst progresses, the walls of the sourcing ellipsoidal crater gradually penetrate into the coal face, and the fractures in the surrounding coal mass also develop continuously, forming channels for gas emission. The formation of fractures requires a finite time with this controlled by many factors. Moreover, the factors controlling gas flow in the damaged coal are ill-constrained, rendering it difficult to derive the gas emission rate from the crater wall directly.

A relationship between the gas emission rate emanating from the crater wall and time may be defined numerically (Hu and Wen, 2013). The veracity of this method is verified by comparation with the results observed in outbursts, shown in Table 1.

Thus, to obtain the gas emission rate, a numerical model of the outburst hole may be established. Based on the above case data, it is found that there is a relationship between the gas emitted from the crater wall and that from the outburst coal, shown in Fig. 3.

Apparent from Fig. 3 is that there is a strong linear relationship between Q_1 and Q_2, fitted as:

$$Q_2 = 11.81Q_1 - 43335.65 \tag{11}$$

then, the total gas emission Q is:

$$Q = 12.81Q_1 - 43335.65. \tag{12}$$

Taking the derivative of the time t on both sides of Eq. (12), the total gas emission rate q can be obtained as:

$$q = 12.81q_1 \tag{13}$$

Incorporating Eq. (10) into the above equation, the total gas emission rate can be obtained:

$$q = \begin{cases} \dfrac{76.86Mv_1}{t_0^2}\left[\dfrac{t-t^2/t_0}{K_n-1} - \dfrac{(t+1)^{2-K_n}-\left(1-2t/t_0\right)}{(K_n-1)(2-K_n)} + \dfrac{2(t+1)^{3-K_n}-2}{(K_n-1)(2-K_n)(3-K_n)t_0}\right] \\ \quad + \dfrac{p_m\phi_m}{p_0\rho}\dfrac{76.86M}{t_0^2}\left(t-\dfrac{t^2}{t_0}\right), t \le t_0 \\ \dfrac{76.86Mv_1}{t_0^2}\left[\dfrac{2(t+1)^{3-K_n}-2(t-t_0+1)^{3-K_n}}{(K_n-1)(2-K_n)(3-K_n)t_0} - \dfrac{(t-t_0+1)^{2-K_n}+(t+1)^{2-K_n}}{(K_n-1)(2-K_n)}\right], t > t_0 \end{cases} \tag{14}$$

3. Contribution of desorptive gas in outbursts

Zhao et al. (Zhao et al., 2016) demonstrated that the expansion energy of the desorbing gas, required for coal transport, is nearly 6.3 times greater than that available from the free gas. This is based on the Zhongliangshan outburst test, the sole field simulation in China. Thus, it is concluded that the desorbing gas plays a crucial role in outbursts. Now we can analyze the contribution of the desorbing gas quantitatively and on a sound theoretical basis.

3.1. The ratio of desorbing gas in the total emission

As the major energy source driving the outburst, high-pressure gas is continuously released to maintain a viable pressure gradient and supplement the energy consumed by the work of gas expansion and coal transport. However, the gases emitted from the ejected coal and the crater wall make different contributions to the outburst development.

Taking the outburst test in the Zhongliangshan Coal Mine as the background, the parameters are collected in Table 2.

At least for a single case, gas emissions may be characterized from the data in Fig. 4. After 24 h, the gas emission rate is minimal and the total volume of the emitted gas asymptotes to 38,362 m^3. For the total gas emission, during the initial several seconds of the outburst, the emission rate of gas increases rapidly and reaches a maximum after 23 s. This then drops until at the end of the outburst (t = 39 s) there is still a residual gas emission of nearly 200 m^3/s. This is consistent with the gas concentration variations observed in the roadways and monitored in outbursts that occurred in 2013 and 2014 (Zhao et al., 2016).

Based on the gas emission model during and after an outburst, we can quantitively study the contribution of the desorbing gas. As the model indicates, the source of the gas is divided between two sources: desorbed gas and free gas. The more gas provided the greater the energy and the greater the contribution to outburst development. The gas desorption process takes a finite time, with

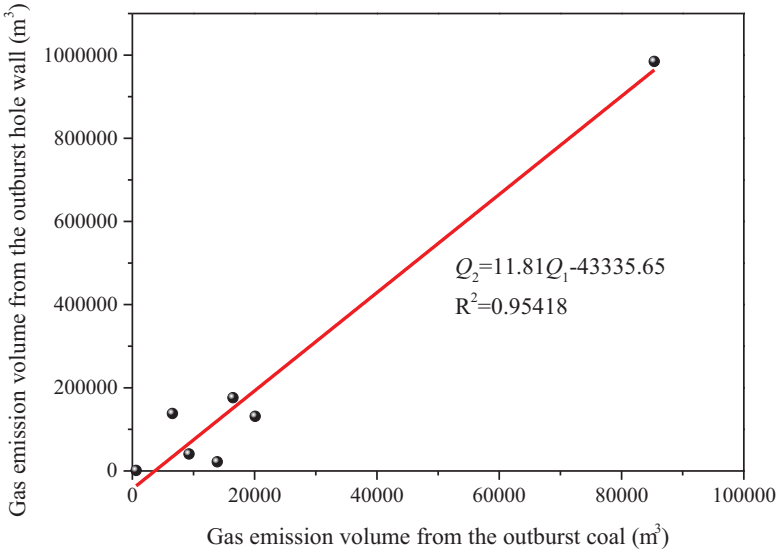

Fig. 3. Fitting of gas emission volumes from the outburst crater wall and that from the outburst coal.

Table 2
Parameters for the test (Zhao et al., 2016).

Outburst intensity M /t	Gas released/m^3	Initial desorption rate v_1/cm^3·(g·s)$^{-1}$	Attenuation coefficient K_n	Gas pressure p_m /MPa	Porosity of coal ϕ_m	Density of coal ρ /t·m^{-3}	Duration of the outburst t_0 /s
817	38540	0.381	1.08	1.75	0.06	1.30	39

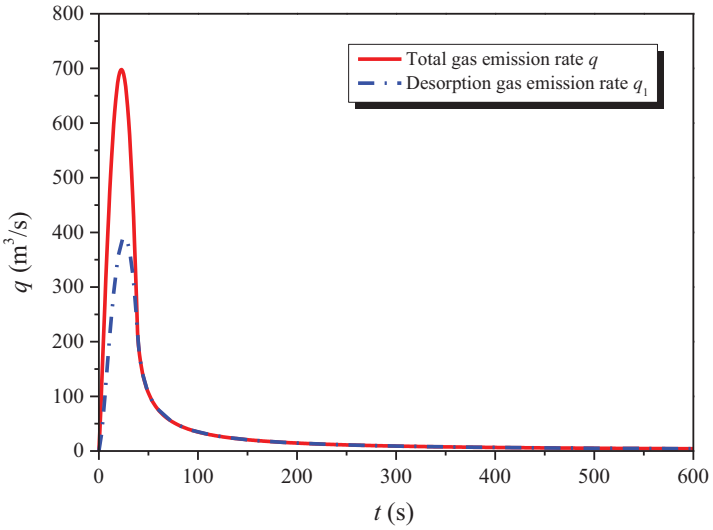

Fig. 4. The gas emission rates measured in the Zhongliangshan outburst test.

a low emission rate at the beginning of the outburst (Fig. 5) that peaks and then falls. It increases drastically following its initiation and exceeds the free gas emission rate at 16.77 s. In the middle stage of the outburst, the proportional increase in the rate of desorption is relatively slow. This is due to the peak period of the ejection of coal with a large amount of free gas instantly emitted. At the termination of the outburst, as the ejected coal mass decreases, a large mass of pulverized coal is actively desorbing - and the gas emission rate again increases rapidly. It is worth noting that after the outburst terminates, fractures in the intact coal will continue to develop in the wall of the crater, and the amount of free gas emission will not drop to zero. In overview, this model adequately represents the two principal sources of gas emission, providing a theoretical basis for quantitative study.

The observation of a high emission rate confirms that a considerable mass of gas has been released but this amount can be directly quantified by the measured cumulative gas emission. Fig. 6 shows the proportional change of cumulative desorbed gas present in the combined mass of the gas emitted. The time when the cumulative mass of desorbed gas exceeds that liberated as free gas is 28.64 s. Within 24 h, 37,776 m^3 of gas is desorbed, accounting for 81.71 % of the total gas. Actually, it is only the gas emission during the outburst that contributes to the development of the outburst. Before 39 s, 10,285 m^3 of gas is desorbed, accounting for 54.89 % of the total amount. As mentioned before, gas emission continues at a considerable rate at the end of the outburst, which will generate a certain degree of pressure and further promote the propagation of the outburst as a two-phase flow.

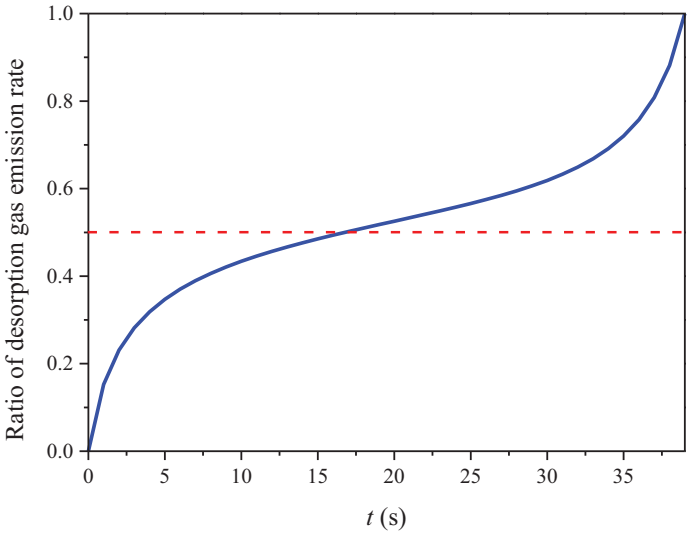

Fig. 5. Proportional change in the desorptive gas emission rate.

3.2. Gas expansion energy

The main form of work of the gas during outburst development is in expansion (Wang et al., 2018a). Eq. (15) represents the work done in expansion by the gas as it transits from the pressure and temperature of state 1 to state 2 under adiabatic conditions (An et al., 2019). If state 2 is the atmospheric state, then it represents the expansion energy of the gas in transiting from state 1 (Eq. (16)). Of course, in the outburst development stage, the gas pressure will not be reduced to atmospheric pressure, but the free and desorbed gas can be compared on this unified basis.

$$W_{ex} = \int_1^2 pdV = \frac{p_2 V_2}{n-1}\left[\left(\frac{p_1}{p_2}\right)^{\frac{n-1}{n}} - 1\right] \tag{15}$$

$$E_{ex} = \frac{p_0 V_0}{n-1}\left[\left(\frac{p_1}{p_0}\right)^{\frac{n-1}{n}} - 1\right] \tag{16}$$

where W_{ex} and E_{ex} represent the expansion work and the expansion energy of the gas, J; p_0 represents the atmospheric pressure, Pa; p_1 and p_2 represent the pressure of gas in states 1 and 2, Pa; V_2 represents the volume of gas under pressure p_2, m^3; n is the adiabatic coefficient, usually taken to be 1.3 for the methane mixture.

From Eq. (16), the expansion energy of the gas is only proportional to the volume of gas under a certain initial pressure. Therefore, the energy contribution of the desorbing gas is the same as in Fig. 6.

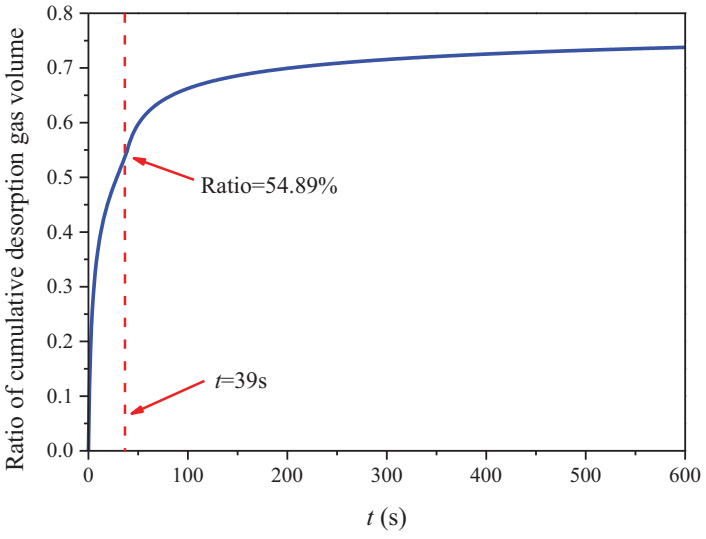

Fig. 6. Proportional change in the cumulative desorption gas volume.

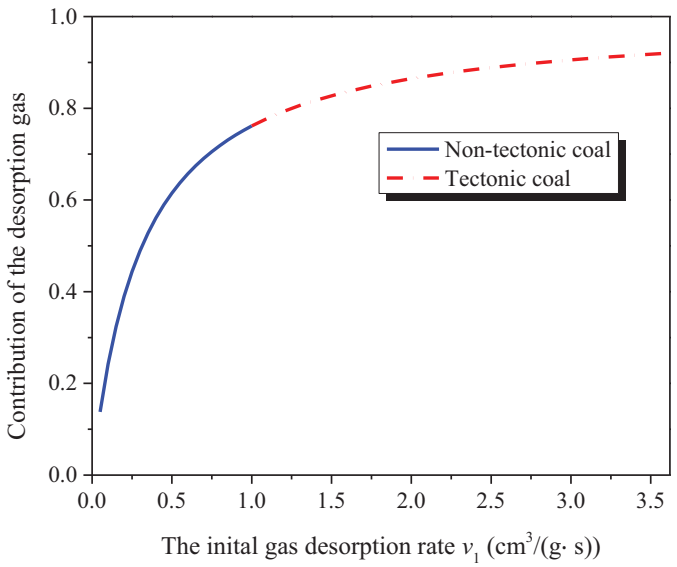

Fig. 7. Influence of initial gas desorption rate on the contribution ratio.

3.3. Influence of initial gas desorption rate

Among all influencing factors, the initial desorption rate is the most important in the contribution to the energy budget of the desorbing gas. Fu et al. (Fu et al., 2008) studied the gas emission characteristics of both tectonic (mylonitized) and non-tectonic coal in the laboratory and obtained Winter-style gas emission rates. Referring to the results, the v_1 of tectonic and non-tectonic coals are 1.00~3.62 $cm^3/(g{\cdot}s)$ and 0.05~1.00 $cm^3/(g{\cdot}s)$, respectively. Accordingly, the contribution of desorption gas during the outburst is shown as Fig. 7.

It can be seen from Fig. 7 that there is a power function relationship between the initial gas desorption rate and the desorption gas contribution ratio. The minimum contribution ratio is 13.77 % and the maximum is 92.06 %. It can be deduced that with the free gas emission unchanged, the desorbing gas plays a decisive role in outburst development. The results also reveals the reasons why coal and gas outbursts are prone to occur near anomalous geological structures.

4. Influence of desorbing gas on gas dynamics of outburst two-phase flow

Although the gas emission model for the outburst test is obtained, the relationship between the pressure and flow rate of the unsteady expansion airflow is unknown - and thus it is impossible to directly determine the gas dynamics of the outburst shock airflow. However, we can use numerical simulation to quantitatively study the pressure transformation and dynamic characteristics for an assumed flow boundary.

4.1. Outbursts without desorption of gas

Since the gas emission model is derived based on the field outburst conditions, the numerical model must be established

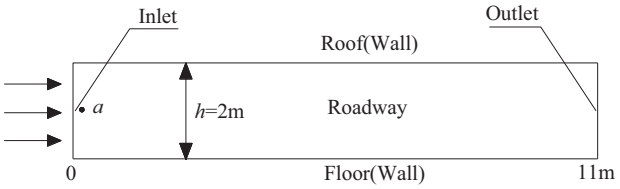

Fig. 8. Physical model of the outburst.

according to the actual size of the roadway. The source of the outburst is simplified as a mass flow inlet, ignoring the formation of the outburst hole. The 2D physical model is shown in Fig. 8.

Firstly, we study the situation without desorption gas emission. In 39 s, 8,453.12 m^3 of free gas is released, with a maximum of 325.12 m^3/s at 19.50 s. The cross-section of the roadway is ~8 m^2, while it is only ~2 m^2 in the 2D model, requiring that the flow rate at the inlet should be scaled by 4 times. The action of the solid phase of the pulverized coal in the outburst flow is important. The density of coal decreases to ~0.56 t/m^3 after crushing, pulverization and swelling (Zhao et al., 2020), and the average volume fraction of coal is 14.72 % during the outburst. Considering the uneven emission, the coal flow is considered to enter the inlet boundary instantaneously with a volume fraction of 20 %.

Point *a*, close to the inlet (0.1 m) in the center of the roadway is selected, and the pressure changes there are shown in Fig. 9. From Fig. 9, in the initial stage of the outburst, with the increase of the gas flowing into the roadway, the pressure of the emission gas increases, since the air in the roadway is almost static. The high-pressure gas accelerates continuously in the roadway until the gas velocity (dynamic pressure) increases to a peak. At 4 s, the gas no longer accumulates, the pressure begins to drop and at this time a shock airflow develops. Due to the continuous influx of gas at the flow inlet, the gas is replenished, and the shock airflow can maintain a high velocity (large dynamic pressure), while the pressure at the inlet remains low. At the termination of the outburst, as the influx of gas gradually decreases to zero, the airflow is difficult to maintain, and the pressure increases as the gas accumulates.

In horizontal flow, the total pressure represents the mechanical energy of the fluid, which is the sum of static pressure and dynamic pressure. Apparent from Fig. 9 is that the total pressure changes and the gas influx law are near consistent - in agreement

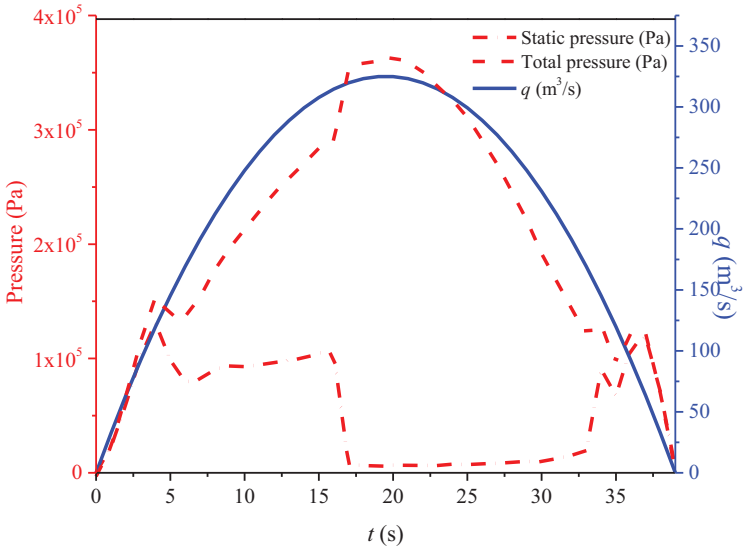

Fig. 9. Gas emission rate and the pressure changes at point *a*.

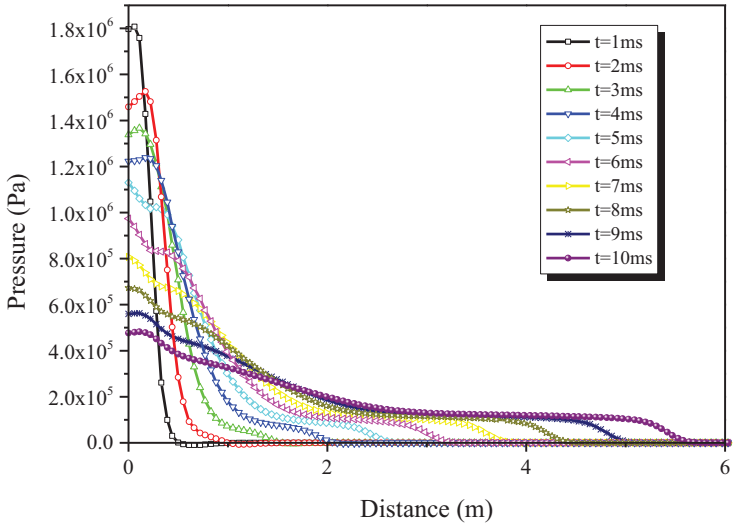

Fig. 10. The pressure distributions in the roadway within the first 10 ms.

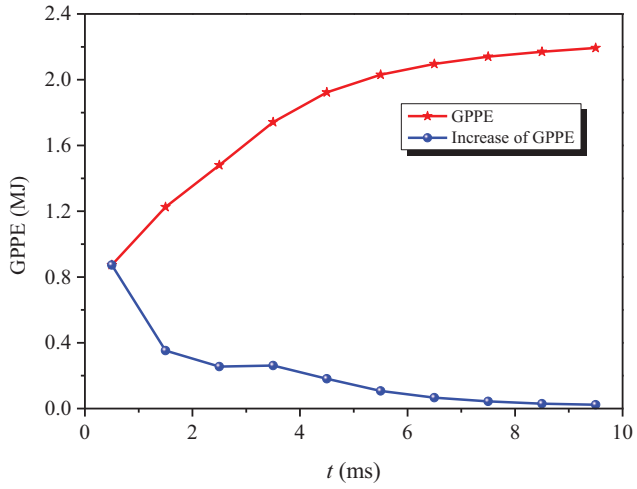

Fig. 11. Evolution of the GPPE with time.

with the conclusions of Section 3.2. At the beginning of the outburst, the velocity of the gas emission is low, and the pressure is nearly equal to the total pressure. As gas flows into the roadway, the pressure increases together with the kinetic energy. We can use the gas pressure potential energy (GPPE) generated in the initial milliseconds to represent the gas-dynamic characteristic of the two-phase outburst flow. However, for the mass flow inlet of gas, the peak gas emission generally occurs in the central stage of the outburst. Based on the above conclusions, a constant inflow of the maximum gas emission rate is adopted. The pressure distributions within 10 ms are shown in Fig. 10.

A method to obtain the gas pressure potential energy E_p has been proposed in previous research (Zhou et al., 2020) and is defined as:

$$E_p = S\int_1^2 pdx \tag{17}$$

where S represents the cross-sectional area of the roadway, being 2 m^2 in the simulations; p represents the pressure in the roadway, Pa; x represents the distance along the roadway, m. The results obtained are shown in Fig. 11.

It can be seen from Fig. 11 that the GPPE generated in the roadway gradually increases due to the gas supplement from the flow inlet. Since the influx is constant, the GPPE should be constant. However, the increment of GPPE decreases with time, indicating that successively more of the GPPE is converted into kinetic energy with time. Thus, it is more reasonable that the GPPE generated in the first millisecond is adopted to represent the dynamic characteristics of the gas in the outburst two-phase flow. Without considering the participation of the desorbing gas, a maximum GPPE of 0.8728 MJ per millisecond is generated by the outburst flow. It is worth noting that such a large pressure will not appear in the outburst, as it is merely a convenient proxy to quantitatively evaluate the energy provided by the maximum gas influx.

4.2. Outbursts considering desorption of gas

As we already know, a large mass of desorbing gas is involved in normal outbursts. The gas emission rates, considering desorption gas and the pressure changes at point *a* are shown in Fig. 12. During the outburst, 18,738.24 m^3 of gas is released, with a maximum of 698.04 m^3/s at 22.79 s. At the completion of the outburst, there is still a considerable influx at the inlet, resulting in the total pressure at point *a* not dropping to zero - there is no section in which the pressure increases.

Similarly, constant gas inflow at the maximum emission rate is used to evaluate the gas-dynamics of the outburst. Although the flow in the simulations is a quarter of the actual value, the pressure distributions in the roadway within the first 10 ms are shown in Fig. 13. Changes in the GPPE with time and derived from the simulation results are shown in Fig. 14. Although the value of GPPE increases monotonically, this increase is close to zero after 4 ms. Moreover, the increase in the GPPE drops much faster than that without considering the desorbing gas. It is apparent that the greater the inflow rate, the faster the conversion of the kinetic energy. Finally, the rate of energy provided by the inflow gas is nearly equal to the conversion rate, resulting in an almost unchanged GPPE. 4.2054 MJ of the GPPE is generated within the first millisecond, which is 4.82 times that without considering the effect of desorbing gas, although the maximum gas emission rate is only 2.15 times larger.

4.3. Influence of initial gas desorption rate

From the previous we infer that the desorptive gas plays crucial role in the propagation of the outburst as a two-phase flow.

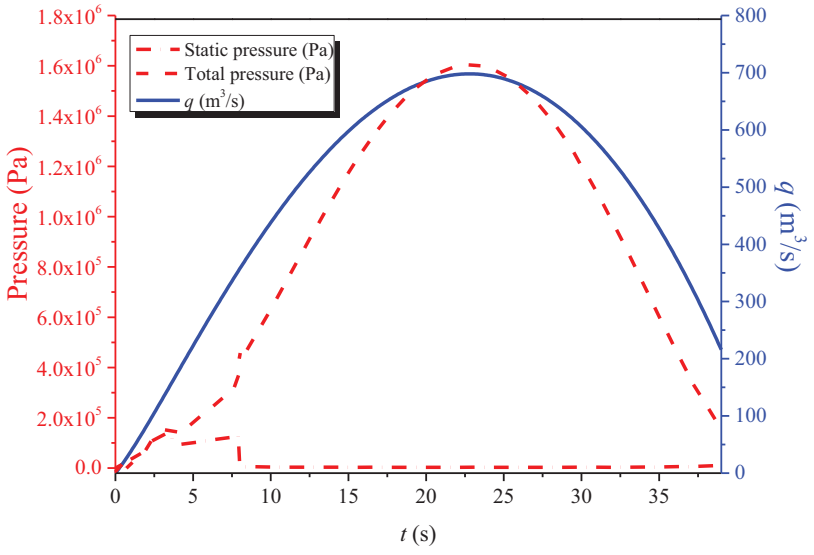

Fig. 12. Gas emission rate and pressure changes at point *a*.

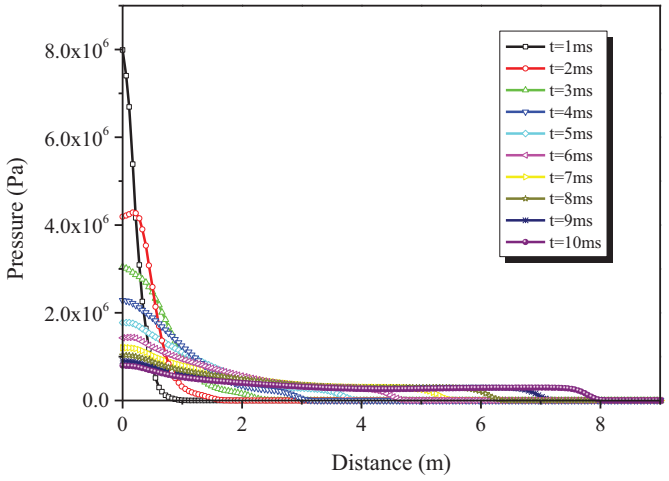

Fig. 13. Pressure distributions in the roadway within the first 10 ms.

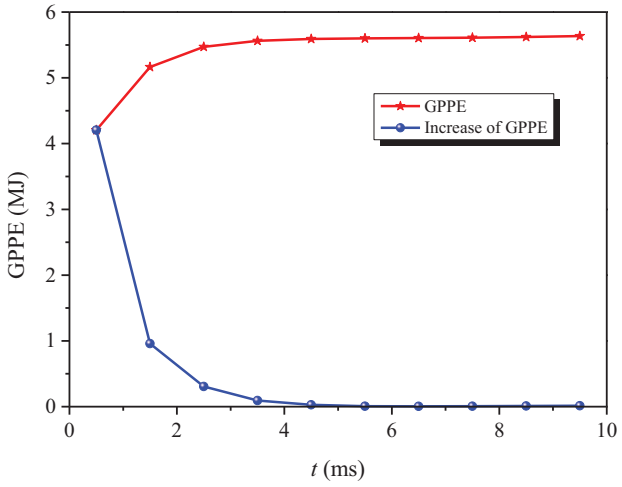

Fig. 14. Evolution of GPPE with time.

The initial gas desorption rate is an important index of gas desorption. To further study its influence on the outburst as a two-phase flow, the average value of the sorption capacity of tectonic coal 1.52 $cm^3/(g{\cdot}s)$ is adopted, as obtained from laboratory experiments (Fu et al., 2008).

The maximum emission rate is 1,856.62 m^3/s at 24.69 s. This is much larger than that with non-tectonic coals. Again, a constant mass flow inlet is used, and the changes in pressure distributions and GPPEs are as shown in Figs. 15 and 16, respectively.

With such a large inflow of the coal-gas mixture, the front of the outburst flow extends beyond the simulation roadway rapidly (within 6 ms). Thus, the magnitudes of the GPPE in only the first 5 milliseconds are available. It can be seen from Fig. 16 that the GPPE is generally decreasing, indicating that the kinetic energy of the shock flow increases so rapidly that the inlet inflow is insufficient to supplement it. In the last several milliseconds, the conversion and the replenishment reach a balance. 16.4896 MJ of GPPE is generated in the first millisecond, which is 3.92 times that with non-tectonic coals. This also explains why outbursts are much more intense in tectonic coals. In fact, it can be speculated that more GPPE is converted in the first millisecond with a larger inflow. Therefore, the actual multiplier in GPPE should be slightly larger than 3.92 and could be determined in simulations with reduced time steps.

The influence of gas desorption on dynamic outburst characteristics is shown in Fig. 17.

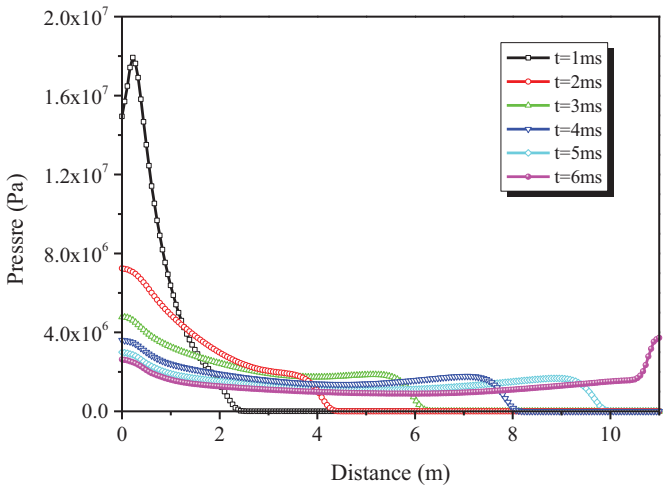

Fig. 15. Pressure distributions along the roadway within the first 6 ms.

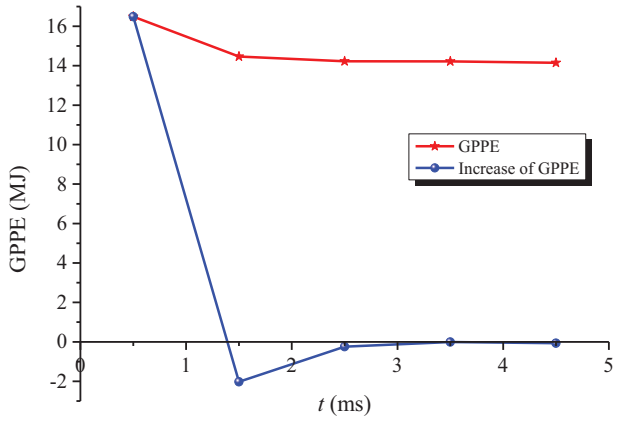

Fig. 16. Evolution of GPPE with time.

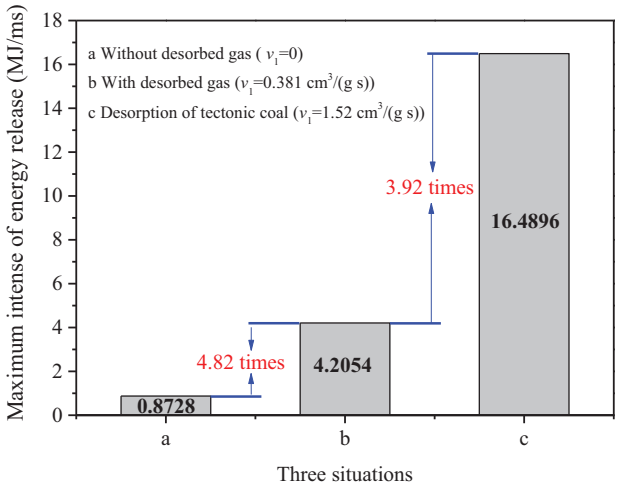

Fig. 17. Influence of gas desorption on dynamic outburst characteristics.

5. Experimental verification and discussion

The important role of gas desorption in the development of outbursts has been established through laboratory experiments (Jin et al., 2018). The energy contribution ratio of the desorbed gas may be obtained from the principle of energy conservation (Fig. 18). The results demonstrate that an average of 56.0 % of the outburst energy

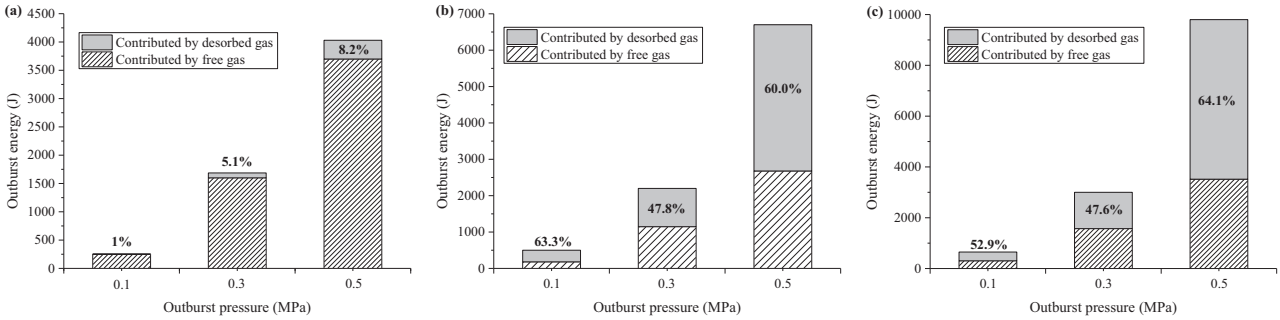

Fig. 18. Energy contribution of free and desorbed gas to the transport of outburst coal. (a) 100 % (1–3 mm coal particle); (b) 33.3 % (< 0.25 mm) and 66.7 % (1–3 mm coal particle); (c) 100 % (< 0.25 mm coal particle).

is provides by the desorbing gas. In this paper, the contribution ratio is 54.89 %, which verifies the gas emission model.

However, outburst simulations in the laboratory are usually performed by filling a chamber with a mixture of pulverized coal and high-pressure gas. The correct form of the mass flow boundary is difficult to replicate under such laboratory conditions. In chamber in experiments, the rate of gas flow increases gradually from this boundary while high-pressure gas is released from the chamber – this results in quite different evolutions in pressure relative to roadways at field scale. Additionally, the duration of outburst experiments is very short (order of 10 s) and the experimental coal sample is only tens of kilograms (Wang et al., 2018b; Yang et al., 2018), cannot provide sufficient intensity in the desorbing gas to promote a true outburst and two-phase flow and cannot fully illustrate the important role of gas desorption. For this reason, Zhao et al. (Zhao et al., 2016) obtained the contribution ratio of 84 % through the analysis of energy conversion in the field outburst case, larger than that in experiments.

Of course, there are some limitations in the derivation of the gas emission model, which need to be improved in subsequent research work. These include:

(1) The law for gas desorption that is used is obtained from pulverized coal under laboratory conditions. Firstly, the coal ejected during field outbursts is a mixture of multiple grain sizes, different from the monodispersed coal particles of single size that are used in the desorption experiments. Secondly, the ejected coal begins in a high-stress/pressure environment, while it is in an atmospheric environment for desorption experiments. Thus, there is a certain deviation between the desorption law that we have used and the actual situation.
(2) The representation of gas emission recovered from the outburst crater wall is simplified. According to relevant research, it is a curve that first stabilizes and then decreases with time, and the total gas emission law should be modified accordingly.
(3) After the outburst terminates, fractures in the coal will continue to develop, leading to continuous emission of the free gas. The contribution of this gas should be incorporated, while there is no release of free gas after the outburst in the model.

6. Conclusions

(1) Based on the analysis of outburst sources, a two-phase coal-gas outburst model is established with a gas emission model during and after outburst defined.
(2) Taking the Zhongliangshan outburst test as an example, the variations in desorbing gas emission rate and cumulative volume are explored. The emission rate of the desorbing gas exceeds that of the free gas at 16.77 s. The cumulative mass of the desorbing gas exceeds the cumulative free gas at later time at 28.64 s.
(3) The contribution of gas desorption to outbursts is analyzed from the perspective of gas expansion energy. This demonstrates that 54.89 % of the expansion energy is provided by desorbing gas. By using the initial gas emission rates measured for both non-tectonic and tectonic coals, there is a power function relationship between the initial gas desorption rate and the desorption gas contribution (13.77 %∼92.06 %), indicating that the desorbing gas plays a decisive role in outburst development.
(4) Taking the gas emission model as a boundary condition, the influence of desorbing gas on dynamic characteristics of the outburst two-phase flow is studied numerically. GPPE released in the first millisecond at the maximum gas emission rate is derived to characterize its effects on the dynamics. The maximum energy release intensity considering gas desorption is 4.82 times that without considering gas desorption for non-tectonic coals. For tectonic (mylonitized) coals the maximum energy release intensity is a further 3.92 times that for non-tectonic coals – principally due to the higher sorbed gas content and due to the rapid release from the fractured coal. This explains why outbursts are much more intense in tectonic coals.

Declaration of Competing Interest

The authors declare that they have no known competing financial interests or personal relationships that could have appeared to influence the work reported in this paper.

Acknowledgements

This research is financially supported by the State Key Research Development Program of China (Grant No. 2018YFC0808101), the National Natural Science Foundation of China (51774292, 51874314, 51604278, 51804312), the Yue Qi Distinguished Scholar Project, China University of Mining & Technology, Beijing, the Yue Qi Young Scholar Project, China University of Mining &Technology, Beijing.

References

An, F., Yuan, Y., Chen, X., Li, Z., Li, L., 2019. Expansion energy of coal gas for the initiation of coal and gas outbursts. Fuel 235, 551–557.
Beamish, B.B., Crosdale, J.P., 1998. Instantaneous outbursts in underground coal mines: an overview and association with coal type. Int. J. Coal Geol. 35, 27–55.
Cao, J., Dai, L., Sun, H., Wang, B., Zhao, B., Yang, X., Zhao, X., Guo, P., 2019. Experimental study of the impact of gas adsorption on coal and gas outburst dynamic effects. Process Safe. Environ. 128, 158–166.
Cao, W., Shi, J.-Q., Durucan, S., Si, G., Korre, A., 2020. Gas-driven rapid fracture propagation under unloading conditions in coal and gas outbursts. Int. J. Rock Mech. Min., 130.
Chen, H., Qi, H., Long, R., Zhang, M., 2012. Research on 10-year tendency of China coal mine accidents and the characteristics of human factors. Safety Sci. 50, 745–750.

Díaz Aguado, M.B., González Nicieza, C., 2007. Control and prevention of gas outbursts in coal mines, Riosa–Olloniego coalfield, Spain. Int. J. Coal Geol. 69, 253–266.
Fedorchenko, A.I., Fedorov, V.A., 2012. Gas-dynamic stage of the coal and gas outburst with allowance for desorption. J. Min. Sci. 48, 15–26.
Fisne, A., Esen, O., 2014. Coal and gas outburst hazard in Zonguldak Coal Basin of Turkey, and association with geological parameters. Nat. Hazards 74, 1363–1390.
Fu, X., Wang, K., Yang, T., 2008. Gas irradiation feature of tectonic coal. J. China Coal Soc. 33, 775–779.
Fu, G., Xie, X., Jia, Q., Tong, W., Ge, Y., 2020. Accidents analysis and prevention of coal and gas outburst- understanding human errors in accidents. Process Saf. Environ. 134, 1–23.
Guan, P., Wang, H., Zhang, Y., 2009. Mechanism of instantaneous coal outbursts. Geology 37, 915–918.
Hu, Q., Wen, G., 2013. The Mechanics Mechanism of Coal and Gas Outbursts. Science Press, Beijing, China.
Jin, K., Cheng, Y., Ren, T., Zhao, W., Tu, Q., Dong, J., Wang, Z., Hu, B., 2018. Experimental investigation on the formation and transport mechanism of outburst coal-gas flow: implications for the role of gas desorption in the development stage of outburst. Int. J. Coal Geol. 194, 45–58.
Karacan, C.Ö., Ruiz, F.A., Cotè, M., Phipps, S., 2011. Coal mine methane: a review of capture and utilization practices with benefits to mining safety and to greenhouse gas reduction. Int. J. Coal Geol. 86, 121–156.
Lama, R.D., Bodziony, J., 1998. Management of outburst in underground coal mines. Int. J. Coal Geol. 35, 83–115.
Li, Z., Wang, E., Ou, J., Liu, Z., 2015. Hazard evaluation of coal and gas outbursts in a coal-mine roadway based on logistic regression model. Int. J. Rock Mech. Min. 80, 185–195.
Liu, H., Lin, B., Mou, J., Yang, W., 2018. Mechanical evolution mechanism of coal and gas outburst. Rock Mech. Rock Eng. 52, 1591–1597.
Nie, B., Ma, Y., Hu, S., Meng, J., 2019. Laboratory study phenomenon of coal and gas outburst based on a mid-scale simulation system. Sci. Rep.-U. K., 9.
Rudakov, D., Sobolev, V., 2019. A mathematical model of gas flow during coal outburst initiation. Int. J. Min. Sci. Technol. 29, 791–796.
Sun, D., Hu, Q., Miao, F., 2012. Motion state of coal-gas flow in the process of outburst. J. China Coal Soc. 37, 452–458.
Sun, H.T., Cao, J., Li, M.H., Zhao, X.S., Dai, L.C., Sun, D.L., Wang, B., Zhai, B.N., 2018. Experimental research on the impactive dynamic effect of gas-pulverized coal of coal and gas outburst. Energies, 11.
Tu, Q., Cheng, Y., Liu, Q., Guo, P., Wang, L., Li, W., Jiang, J., 2018. Investigation of the formation mechanism of coal spallation through the cross-coupling relations of multiple physical processes. Int. J. Rock Mech. Min. 105, 133–144.
Wang, C., Yang, S., Li, J., Li, X., Jiang, C., 2018a. Influence of coal moisture on initial gas desorption and gas-release energy characteristics. Fuel 232, 351–361.
Wang, C., Yang, S., Yang, D., Li, X., Jiang, C., 2018b. Experimental analysis of the intensity and evolution of coal and gas outbursts. Fuel 226, 252–262.
Wang, C., Yang, S., Li, X., Li, J., Jiang, C., 2019. Comparison of the initial gas desorption and gas-release energy characteristics from tectonically-deformed and primary-undeformed coal. Fuel 238, 66–74.
Wang, K., Zhou, A., 2014. The Catastrophic Law of Coal and Gas Outbursts. China University of Mining and Technology Press, Xuzhou, China.
Yang, D., Chen, Y., Tang, J., Li, X., Jiang, C., Wang, C., Zhang, C., 2018. Experimental research into the relationship between initial gas release and coal-gas outbursts. J. Nat. Gas Sci. Eng. 50, 157–165.
Zhang, J., Xu, K., Reniers, G., You, G., 2020. Statistical analysis the characteristics of extraordinarily severe coal mine accidents (ESCMAs) in China from 1950 to 2018. Process Saf. Environ. 133, 332–340.
Zhao, W., Cheng, Y., Jiang, H., Jin, K., Wang, H., Wang, L., 2016. Role of the rapid gas desorption of coal powders in the development stage of outbursts. J. Nat. Gas Sci. Eng. 28, 491–501.
Zhao, W., Cheng, Y., Guo, P., Jin, K., Tu, Q., Wang, H., 2017. An analysis of the gas-solid plug flow formation: new insights into the coal failure process during coal and gas outbursts. Powder Technol. 305, 39–47.
Zhao, W., Cheng, Y., Pan, Z., Wang, K., Liu, S., 2019. Gas diffusion in coal particles: a review of mathematical models and their applications. Fuel 252, 77–100.
Zhao, W., Cheng, Y., Wang, K., 2020. Theory and Application of Gas Diffusion in Coal. China University of Mining and Technology Press, Xuzhou, China.
Zhi, S., Elsworth, D., 2016. The role of gas desorption on gas outbursts in underground mining of coal. Geomech. Geophys. Geo-Energy Geo-Resour. 2, 151–171.
Zhou, A., Wang, K., Feng, T., Wang, J., Zhao, W., 2018. Effects of fast-desorbed gas on the propagation characteristics of outburst shock waves and gas flows in underground roadways. Process Saf. Environ. 119, 295–303.
Zhou, A., Zhang, M., Wang, K., Zhang, X., Feng, T., 2020. Quantitative study on gas dynamic characteristics of two-phase gas-solid flow in coal and gas outbursts. Process Saf. Environ. 139, 251–261.